The University of
Nottingham

UNITED KINGDOM · CHINA · MALAYSIA

Tyler, Bonnie J. and Hook, Andrew L. and Pelster, Andreas and Williams, Paul and Alexander, Morgan R. and Arlinghaus, Heinrich F. (2017) Development and characterization of a stable adhesive bond between a poly(dimethylsiloxane) catheter material and a bacterial biofilm resistant acrylate polymer coating. Biointerphases, 12 (2). 02C412/1-02C412/12. ISSN 1559-4106

Access from the University of Nottingham repository:
http://eprints.nottingham.ac.uk/44396/1/Development%20and%20characterization%20of %20a%20stable%20adhesive%20bond%20between%20a%20poly%28dimethylsiloxane %29%20catheter%20material%20and%20a%20bacterial%20biofilm%20resistant %20acrylate%20polymer%20coating.pdf

Development and characterization of a stable adhesive bond between a poly(dimethylsiloxane) catheter material and a bacterial biofilm resistant acrylate polymer coating

Bonnie J Tyler, Andrew L Hook, Andreas Pelster, Heinrich F Arlinghaus, Paul Williams and Morgan R Alexander

Abstract:

Catheter associated urinary tract infections (CA-UTIs) are the most common health related infections world wide, contributing significantly to patient morbidity and mortality and increased health care costs. To reduce the incidence of these infections, new materials that resist bacterial biofilm formation are needed. A composite catheter material, consisting of bulk PDMS coated with a novel bacterial biofilm resistant polyacrylate (EGDPEA–co-DEGMA) has been proposed. The coated material shows excellent bacterial resistance when compared to commercial catheter materials but delamination of the coatings under mechanical stress presents a challenge. In this work, the use of oxygen plasma treatment to improve the wettability and reactivity of the PDMS catheter material and improve adhesion with the EGDPEA–co-DEGMA coating has been investigated. Argon Cluster 3D-imaging Time-of-Flight Secondary Ion Mass Spectrometry (ToF-SIMS) has been used to probe the buried adhesive interface between the EGDPEA–co-DEGMA coating and the treated PDMS. ToF-SIMS analysis was performed in both dry and frozen-hydrated states and results were compared to mechanical tests. From the ToF-SIMS data we have been able to observe the presence of PDMS, silicates, salt particles, cracks and water at the adhesive interface. In the dry catheters, low molecular weight PDMS oligomers at the interface were associated with poor adhesion. When hydrated, the hydrophilic silicates attracted water to the interface and led to easy delamination of the coating. The best adhesion results, under hydrated conditions, were obtained using a combination of 5 min O_2 plasma treatment and silane primers. Cryo-ToF-SIMS analysis of the hydrated catheter material showed that the bond between the primed PDMS catheter and the EGDPEA–co-DEGMA coating was stable in the presence of water. The resulting catheter material was resisted *Escherichia coli* and *Proteus mirabilis* biofilm colonization by up to 95 % compared with uncoated PDMS after 10 days of continuous bacterial exposure and had the mechanical properties necessary for use as a urinary catheter.

1. Introduction

Catheter associated urinary tract infections (CA-UTIs) are the most common health care related infections worldwide[1] with an estimated 100,000 symptomatic infections annually in the USA alone[2-3]. These CA-UTIs result in increased length of hospital stays with associated costs[4], contribute to development of drug resistant bacterial strains[3], and lead to increased mortality[5-6]. Bacterial biofilm formation on the interior and exterior surfaces of the catheter has been identified as the most important cause of CA-UTIs[7-8]. To reduce the incidence of these infections, there is a critical need for new catheter materials that prevent bacterial biofilm formation. Using a combinatorial polymer library, Hook et al have identified a bacterial biofilm resistant polyacrylate a copolymer of ethylene glycol dicyclopentenyl ether acrylate (EGDPEA) and di(ethyleneglycol) methyl ether methacrylate (DEGMA), that is resistant to bacterial attachment in both *in vitro* and *in vivo* assays[9-10]. This copolymer has mechanical properties compatible with a flexible coating on PDMS necessary for many medical device applications such as catheters[11].

Poly (dimethylsiloxane) has the flexibility, inertness and durability required for urinary catheters as well as a range of other biomedical applications such as breast prosthesis, hydrocephalus shunts, cardiac pacemakers, cochlear implants, artificial skins, temporomandibular joints, drug delivery systems, drainage implants in glaucoma, maxillofacial reconstruction, oesophagus replacements, finger joints, and denture liners. Despite its excellent bulk properties, the surface properties of PDMS frequently lead to an adverse biological response such as fibrotic encapsulation, thrombosis or bacterial biofilm formation[12-14]. For this reason, there have been many efforts to modify the surface of PDMS in order to improve the induced biological response. In this work we have investigated coating PDMS catheter tubing with the EGDPEA–co-DEGMA coating to create a catheter material that would be resistant to bacterial biofilm formation.

Creating a strong adhesive bond between PDMS and any coating is difficult because of the inertness and hydrophobicity of PDMS. A number of strategies have been employed to modify the surface of PDMS, such as blending, copolymerization, interpenetrating polymer networks and functionalization[15-16]. In this work, we have used O_2 plasma treatment of PDMS to improve the hydrophilicity and reactivity of the surface. Plasma treatment has been previously used to reduce the hydrophobicity of PDMS and hence make it more favorable for cell attachment. In particular, O_2 plasma has been extensively investigated for producing a thin silica sheet on PDMS, providing a hydrophilic layer that can prevent solvent swelling, improve wetting and inhibit the migration of PDMS oligomers to the surface. In addition to producing a silica layer, plasma treatment is well known for its ability to produce long-lived, highly reactive radicals within treated species [17]. These groups can be advantageous for establishing covalent links between a coating and the PDMS or for inducing subsequent grafting-to polymerisation [18]. In this study we explore the influence of O_2 plasma treatment on PDMS at improving the interaction of an antibacterial coating [9,10] with PDMS catheter tubing.

Historically, studying adhesion between polymer layers has been extremely challenging because of a lack of suitable analytical techniques for probing the buried interface. Recent advances in cluster ion beam technology have made sputter depth profiling a practical alternative for depth profiling and 3D imaging of organic materials [19-23]. In this work we have used dual-beam 3D imaging Time of Flight secondary ion mass spectrometry (ToF-SIMS) [24], using an argon cluster sputter source, to probe the adhesive layer between the EGDPEA–co-DEGMA coating and a PDMS catheter in order to better understand and thereby improve the adhesion.

2. Methods

A. Polymer preparation

To form the polymer, Bis[(difluoroboryl)diphenylglyoximato]cobalt(II) (CoPhBF, 1000ppm) and 2,2'-azobis(4-methoxy-2,4-dimethylvaleronitrile) (0.5%, w/v) were added to monomer (ethylene glycol dicyclopentenyl ether acrylate (EGDEA) and di(ethyleneglycol) methyl ether methacrylate (DEGMA) EGDEA:DEGMA = 3:1 in toluene. The chemical structure of the monomers is shown in figure S1 in the supplemental material. The ratio between monomers and toluene was 1:4. The solution was degassed using at least two freeze-pump-thaw cycles, until no more bubble formation was observed in the thaw step. The polymerisation was conducted at 80 °C for 24 h under N_2. The polymerization was terminated by exposure to air and cooling the reaction flask. ^1H and ^{13}C nuclear magnetic resonance (NMR) spectra were acquired in deuterated chloroform on both Bruker DPX (300 MHz) and AV (400 MHz) instruments. Number-average molecular weight (Mn), weight-average molecular weight (Mw), and polydispersity (PD) were obtained by gel permeation chromatography (GPC) with

a fitted IR detector. Polymer samples (7 mg/ml) dissolved in tetrahydrofuran were flowed (1 ml/min) through a PLgel 5 mm guard column (Polymer Laboratories) and two PLgel 5mm MIXED-C columns (Polymer Laboratories) at 40 °C. Polymer was precipitated by dropwise addition to cold hexane. The polymer was dried under vacuum (<50 mbar) overnight before use.

B. Sample preparation

PDMS tubing (Sterilin) of 100% was cut into approximately 10 mm lengths, washed in acetone for 10 minutes with sonication, dried and then O_2 plasma treated using a custom built reactor as shown in figure 1. The reactor pressure was initially reduced to below 0.02 mbar and flushed twice with O_2 before plasma treatment. For plasma treatment O_2 initial pressure was 0.4 mbar and typically running pressure was 0.49-0.58 mbar. Plasma treatment times were 10 s, 1 min., 5 min., 10 min. and 30 min. Plasma power was 100 W. After plasma treatment was completed the chamber was evacuated to below 0.08 mbar before exposure to atmosphere. The treated samples were then immersed for 10 min. into 7.5% (w/v) polymer solution in dichloromethane within 2 min. from the end of the plasma cycle. Samples were then withdrawn at approximately 5 mm/s, blotted and dried overnight at ambient conditions and then dried in vacuum (<50 mbar) at 75 ºC for 3 days.
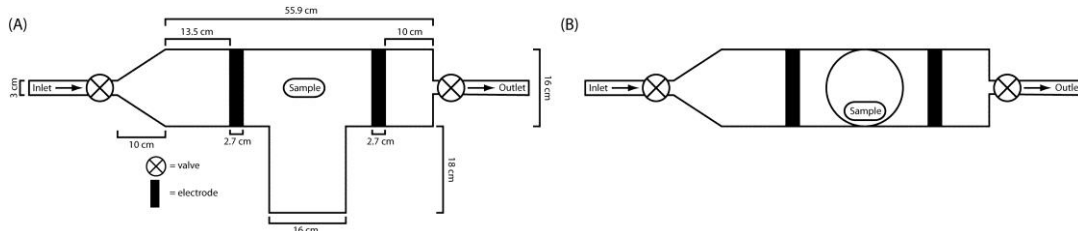

Figure 1. Schematic depiction of the plasma reactor (A) top view and (B) side view.

Silane primed samples were prepared by immersing PDMS tubing (Sterilin) into a 20% (v/v) mixture of tetrabutyl-titanate, tetrapropylsilicate and tetra (2-methoxyethoxy) silane in naphtha solvent (Nusil MED1-161). Samples were withdrawn at approximately 1 mm/s and allowed to dry for 5 mins before dipping into 7.5% (w/v) polymer solution in dichloromethane. Samples were then withdrawn at approximately 5 mm/s, blotted and dried overnight at ambient conditions and then dried in vacuum (<50 mbar) at 75 ºC for 3 days.

C. Sample analysis

Samples were assessed gravimetrically before and after coating. For measurements of water contact angle (WCA) a CAM200 instrument (KSV Instruments, Ltd) was used to dispense 10 µL volume sessile water droplets onto plasma treated PDMS samples. Three measurements were taken per sample. Ultrapure water was used for all CA measurements (18.2 MΩ resistivity at 25 °C). WCA measurements after O_2 plasma treatment were taken within 2-4 min. of the completion of the plasma treatment cycle. Light microscopy images were acquired using an Olympus IX51 microscope and a Smart Imaging System (IMSTAR S.A.) with a 10 × objective lens. Scanning electron microscopy images were acquired using a JSM 6400 Scanning Microscope (Jeol Winsem). Samples were fixed onto conductive carbon tape and pre-coated with an approximately 10 nm Pt layer prior to imaging. For cross-sectional images samples were immersed into liquid nitrogen and then fractured using a scalpel blade.

D. Revolutions-to-delamination assay

To assess the strength of the interface between the polymer coating and PDMS substrate, coated samples were subjected to a rolling tube compression test which put very stringent interfacial stresses upon the interfaces. The output from this was the number of revolutions to delamination (RTD) which could be compared as a measure of interfacial stability. The test was performed by placing the samples between two glass slides and a 1 kg weight was placed on top of the sample (see supplemental material, fig. S2). The bottom glass slide was fixed whilst the top slide was moved back and forth to cause the sample to roll along the two glass surfaces. The sample was rolled until a complete revolution was completed and then the movement direction was reversed. This was continued until a delamination event was observed or 1000 rotations were completed. Between samples both glass surfaces were thoroughly cleaned with isopropanol. For analysis of hydration effects, samples were placed into ultrapure water (18.2 MΩ resistivity at 25 °C) for 1 h. Samples were then blotted onto paper towel to remove excess water from the lumen of the sample and then rolled once to remove excess water from the exterior of the sample.

E. Bacterial attachment assay

Uropathogenic *Escherichia coli* (UPEC) (*E. coli* 536)[25] and *Proteus mirabilis* (DSMZ226637, clinical isolate, Queens Medical Centre, UK) were routinely grown on either LB (Luria-Bertani, Oxoid, UK) agar plates at 37 °C or in broth at 37 °C with 200 rpm shaking. RPMI-1640 chemically defined medium (Sigma, UK) was used in the biofilm experiments. Prior to incubation with the bacteria, the coated samples were UV sterilised and washed in phosphate buffer saline (PBS, Oxoid) for 10 min. Bacteria were grown on polymer samples under similar conditions to those previously described[12]. Briefly, samples were incubated in 10 ml medium inoculated with diluted (OD_{600} = 0.01) bacteria from overnight cultures and grown at 37 °C with 60 rpm shaking for 3-10 days. After 3 days of growth the media was decanted and replaced with 10 ml of fresh, pre-warmed media. As growth medium controls, coated samples were also incubated without bacteria. At the desired time points, the samples were removed, washed three times with 15 ml PBS at room temperature for 5 min.at 60 rpm, rinsed with distilled H_2O and stained with 20 µM SYTO17 dye (Invitrogen, UK) at room temperature for 30 min. After air drying, the samples were examined using a Carl Zeiss LSM 700 Laser Scanning Microscope with ZEN 2009 imaging software (Carl Zeiss, Germany). The coverage of bacteria on the surface was analysed using open source Image J 1.44 software (National Institute of Health, USA).

F. ToF-SIMS Analysis

ToF-SIMS measurements were performed on a custom built ToF-SIMS instrument which is largely comparable to the IONTOF V. The instrument is equipped with a novel cryo-preparation chamber to allow easy handling of frozen hydrated samples. The 3D images of the catheters were obtained in dual beam mode using an approximately 0.05 pA (pulsed mode) 30 keV Bi_3^+ primary ion beam for analysis and 2.1 nA, 10 keV Ar_{2000}^+ for sputtering. Non-interlaced sputtering, with a 50 s analysis cycle, 20 s sputter cycle, and 1 s pause, was used to minimize sample charging.

To study hydration effects, samples were submerged in ultrapure water for >1 hr. The sample was then blotted dry, mounted on a copper stub and plunge-frozen in liquid nitrogen. Freezing was performed inside a glove box that is attached to the ToF-SIMS cryo-preparation chamber so that samples could be introduced to the vacuum without formation of a frost layer on the surface. Once

transferred to the instrument, the samples were maintained at -130 °C throughout the analysis process.

3. Results and Discussion

A. Plasma treatment of PDMS

PDMS samples were initially exposed to O_2 plasma treatment at a power of 100 W from 10 s – 30 mins. After treatment samples were assessed by light microscopy and WCA. Figure 2 shows the light micrographs of untreated PDMS (fig. 2A) and samples treated with O_2 plasma for 5 min.(fig. 2B), 10 min.(fig. 2C) and 30 min.(fig. 2D). No change in the appearance of samples was observed after plasma treatment for 10 s or 1 min. compared with untreated PDMS. After 5 minutes treatment, cracks were observed on the PDMS surface (fig. 2B). The number of cracks increased with further increases in treatment (fig. 2 C-D). Crack formation has previously been observed after plasma treatment of PDMS due to the formation of a brittle silica layer, which becomes thicker with longer treatment times [14, 26-28].
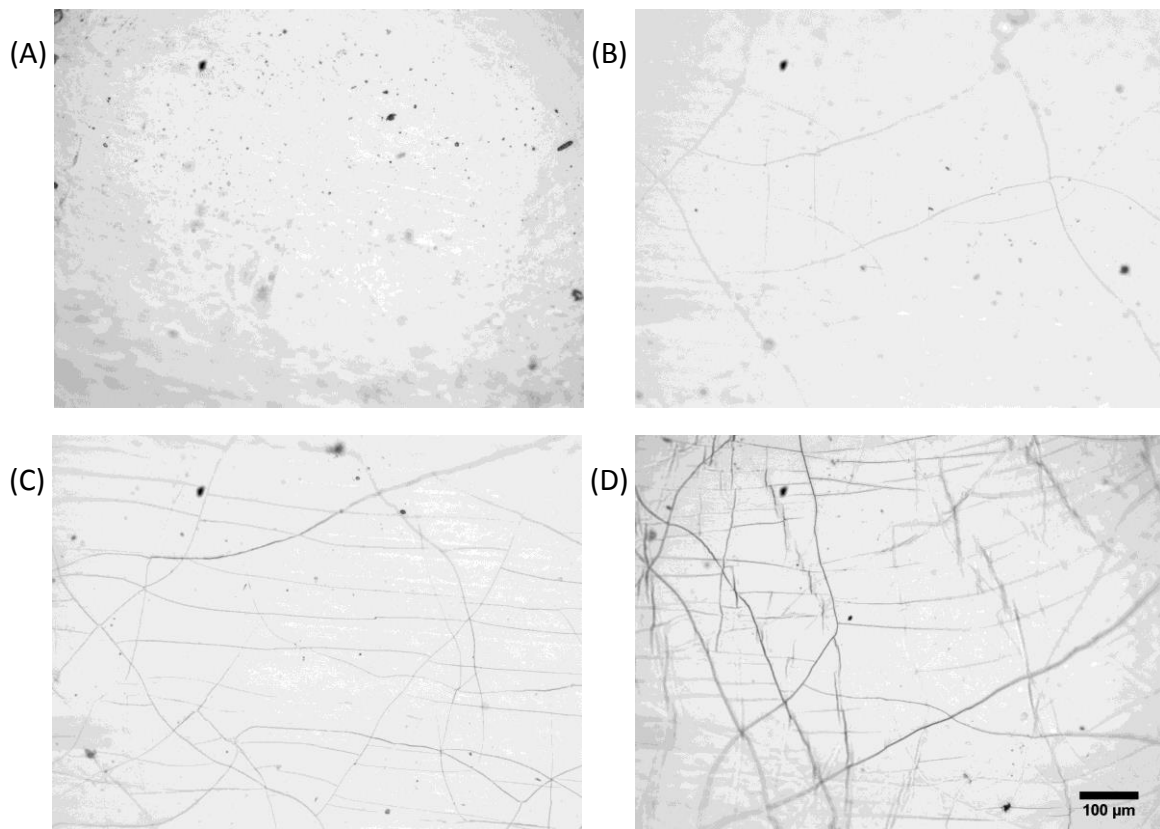

Figure 2. Bright field light microscopy images of PDMS after oxygen plasma treatment. Treatment times were (A) as received, (B) 5 min, (C) 10 min, and (D) 30 min.

Figure 3 shows water contact angle measurements for the plasma treated PDMS immediately (2-4 minutes) following plasma treatment (fig. 3A) and 1 week after treatment (fig. 3B). Immediately following plasma treatment, the WCA (measured within 5 mins from treatment) decreased from 116 ± 2° to 65 ± 2 ° for samples that were plasma treated between 1 and 10 minutes. For the 30 minute plasma treatment, a higher WCA of 91° ± 3° was observed, which correlated with increased cracking of the sample surface. After 1 week, the WCA of all the samples (fig. 3B) was within measurement error of the untreated PDMS. Hydrophobic recovery of treated PDMS has been

previously observed in many studies and has been attributed to migration of lower molecular weight PDMS oligomers from the bulk to the surface.
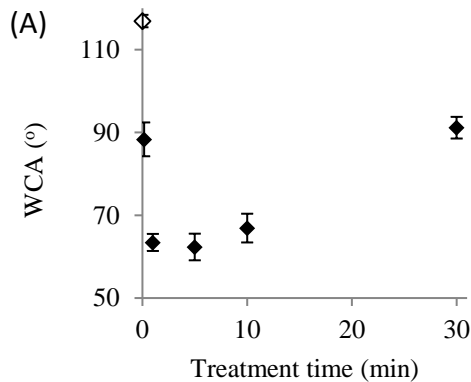

Figure 3. Change in WCA of the oxygen plasma treated time immediately after plasma treatment. The unfilled symbol indicates untreated PDMS.

B. Substrate coating

After plasma treatment, the catheter tubing was dip-coated with EGDPEA–co-DEGMA. Once dried, all coatings on plasma treated PDMS appeared smooth and homogeneous. In contrast, coatings on untreated PDMS dewetted on the surface. The shortest treatment time (10 s) was thus sufficient to avoid dewetting of the coating. The coating thickness was determined by gravimetric analysis and SEM measurements and is shown in figure 4, representative SEM image shown in the supplemental material fig S3. A maximum thickness of 7 ± 1 µm was observed for the 5 minute treatment time. Coating thickness decreased with an increase in treatment time to a minimum thickness of 2 ± 0.5 µm for the 30 minute treatment (fig. 4A). SEM measurements of the coating thickness (fig. 4B), however, show large variability (std > ± 4 µm) in the coating thickness for all treatment times. It should be noted that the gravimetric analysis measures an average thickness across the whole sample whereas the SEM measurements are associated with localised regions of the sample.
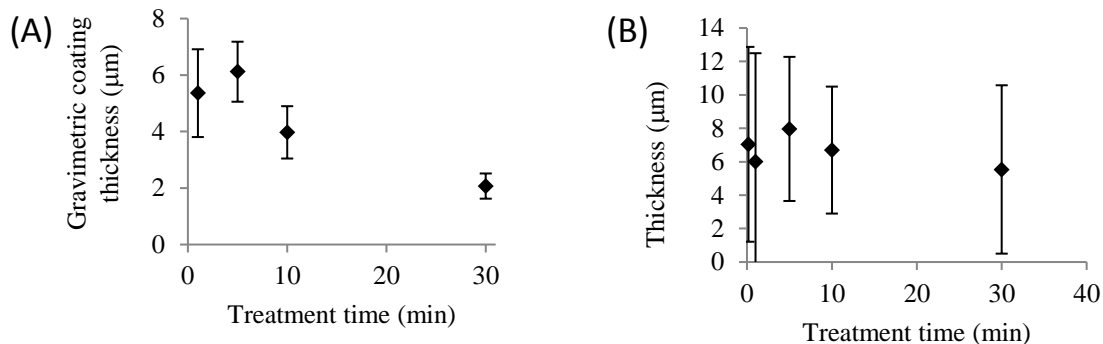

Figure 4. Coating thickness as determined by gravimetric analysis (A) and SEM measurements (B). Error bars equal ± 1 standard deviation unit, n = 5.

C. Mechanical testing

Figure 5 shows the result of the loaded roll test for dry and hydrated samples. Examples of delamination events are shown in the supplemental material (fig. S4). For dry samples, the RTD increased from less than 10 for treatment times under 5 minutes to >1000 for treatment times over 10 minutes (fig. 5A). Note that the test was stopped after 1000 revolutions if no delamination occurred so the apparent plateau in figure 5 is artificial. A dramatic reduction in adhesion was observed after hydration, with the maximum RTD of 12 ± 7 occurring for a treatment time of 5 mins. This suggests that this treatment time produced sufficient reactivity at the PDMS surface to ensure adhesion between the coating and the catheter without excessive production of a silica layer. Further increasing the treatment time to 10 min. decreased the RTD to 2 revolutions, and a further increase to 0.5 revolutions was observed for a treatment time of 30 mins.
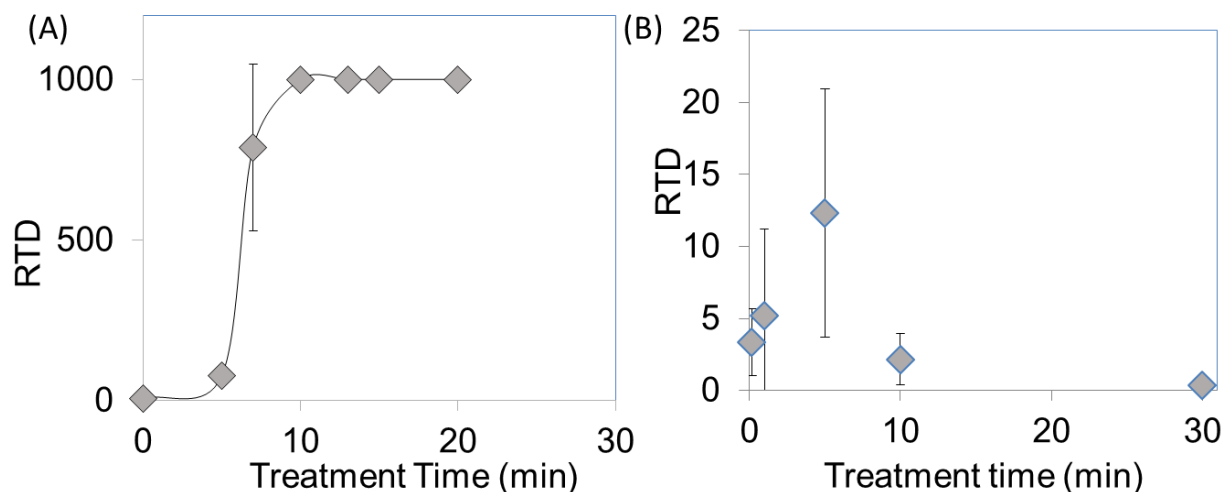

Figure 5: RTD observed for various O_2 plasma treatment times for dry (A) and hydrated (B) EGDPEA-co-DEGMA coated PDMS catheter samples. Error bars equal ± 1 standard deviation unit, n = 5.

D. Bacterial attachment assay

A treatment time of 5 min. was selected for bacterial attachment studies because it showed the best resistance to delamination under hydrated conditions. These coatings were subjected to bacterial attachment assays using UPEC and *P. mirabilis* for 3-10 days. These two bacterial strains are highly relevant in catheter associated urinary tract infections [29-30]. Results of the bacterial attachment assay are shown in figure 6. After 3 days culture (fig. 6A) bacterial coverage on the poly(EGDPEA-co-DEGMA) was < 3% and < 1.5% for *P. mirabilis* and UPEC, respectively. This compares with *P. mirabilis* coverage of > 17% and UPEC coverage of > 6% for the untreated and silver hydrogel controls. The low bacterial coverage on the EGDPEA–co-DEGMA coating was maintained for the entire 10 days incubation period (fig. 6A&C). Samples showed no signs of delamination throughout this period, demonstrating that the oxygen plasma treatment produced a sufficiently strong interface between the coating and PDMS to prevent delamination in an aqueous environment. On the untreated PDMS the *P. mirabilis* coverage remained steady at approximately 23% for the 10 day period whilst the UPEC coverage increased from 6% to > 30% from 3 to 10 days incubation. After 3 days the *P. mirabilis* coverage on the silver hydrogel was > 17%, however, this decreased to approximately 5% after 10 days suggesting that the silver hydrogel may have been able to kill this bacterial species over the time course of the experiment. The UPEC coverage on the silver hydrogel catheter fluctuated throughout the experiment within the range of 12-35%. In

summary, the EGDPEA–co-DEGMA coating achieved between 86-95% reduction in bacteria coverage (*P. mirabilis* and UPEC) compared with untreated PDMS and between 66-93% compared with the silver hydrogel after 10 days of continuous bacterial exposure.
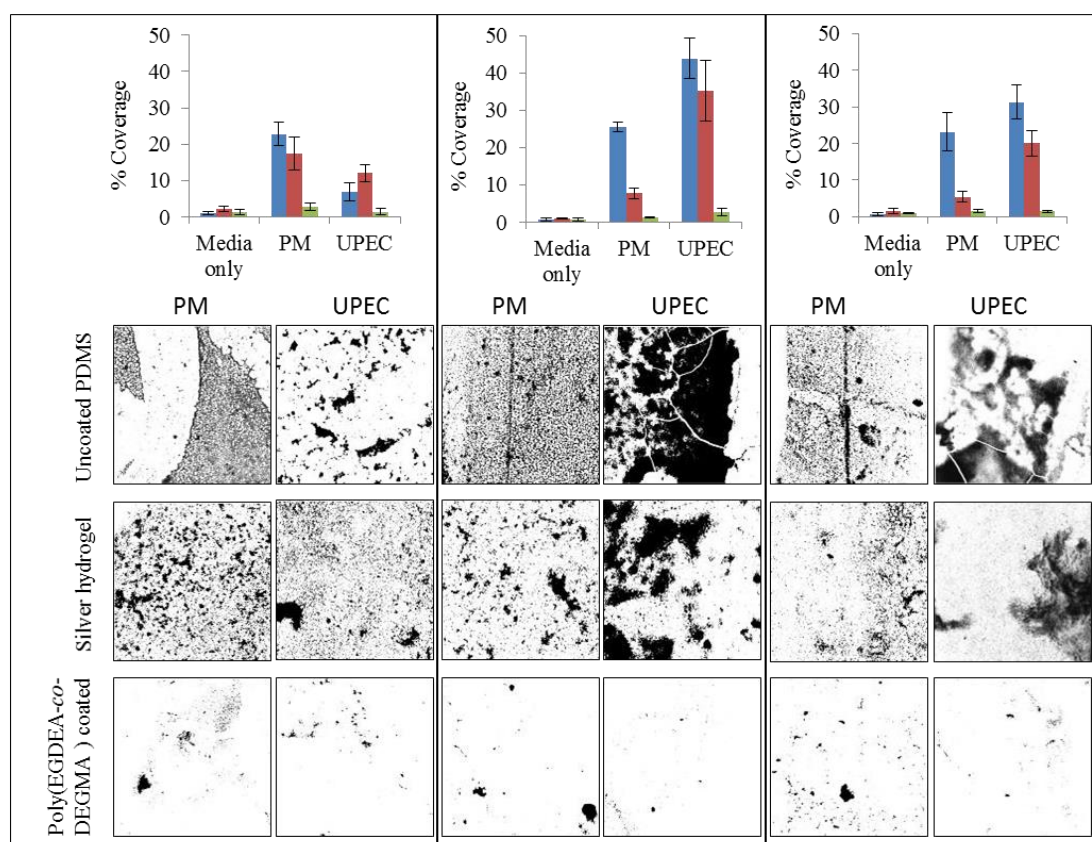

Figure 6. Summary of bacterial attachment onto uncoated PDMS (blue square), silver hydrogel (red square), and poly(EGDPEA-co-DEGMA) coated PDMS (green square). Analysis was performed after (a) 3, (b) 6, or (c) 10 days of culturing of samples with *P. mirabilis* (PM) and UPEC. Bacterial coverage (top) was calculated on SYTO64 stained samples. Three images were acquired from each sample, and three repeated samples were assessed for each time point/same type. Error bars equal ± 1 standard deviation unit, n = 9. The representative maximum z-projection images for each substrate and bacterial species are shown. Images are 640×640 μm².

E. ToF-SIMS Analysis

Replicate ToF-SIMS 3D-images were collected on 100 μm x 100 μm areas on the 5, 10 and 30 min. 100 W O_2 treated samples. The sputter time required to reach the interface varied significantly within each sampled region indicating non-uniformity in either the coating thickness or sputter yield. This non-uniform layer thickness led to poor resolution of the interface. To improve resolution of the interface, all 3D images were corrected to align the layers at the base of the polymer layer [31-32]. Alignment was done using an autocorrelation function rather than a threshold as this proved less sensitive to noise. Note that this pixel level realignment of the ToF-SIMS profiles was intended to improve resolution of the interface rather than produce realistic 3D images. The images were processed using principal components analysis and multivariate curve resolution to identify all major components. Three major components, EGDPEA–co-DEGMA, SiO_n, and PDMS were identified in all of the sampled regions. Additionally, dust particles rich in Na^+, K^+ and NH_4^+ were observed at the interface between the polymer film and the catheter in many of the regions. ToF-SIMS spectra

for these components are in the supplemental material (fig. S5). Salt rich particles are a common component of ambient aerosol[33-34] and their presence at the interface suggest they were most likely present on the catheter surfaces prior to plasma treatment and EGDPEA–co-DEGMA coating.

Representative depth profiles and 3D images of samples treated for 5, 10, and 30 min are shown in Fig. 7. The signals shown are the sum of characteristic peaks determined from the multivariate analysis. A table summarizing these peaks is provided in the supplementary material (Table S1). The unusual drop in the EGDPEA-co-DEGMA signal in the depth profiles, at the outermost surface of the samples, is an artefact of the topographic correction of the data. For all the images, the EGDPEA-co-DEGMA layer is shown in blue, silicate is shown in green, and PDMS is shown in red. All the samples show traces of PDMS contamination at the outermost surface on top of the EGDPEA-co-DEGMA coating.

For the 5 min treated sample [Figs. 7(a) and 7(b)], four layers were identified, the top layer of EGDPEA-co-DEGMA, followed by an ultrathin layer of pure oligomeric PDMS, a layer of mixed silicate and PDMS, and then the bulk cross-linked PDMS catheter material. The sputter ion yield for silicates with argon cluster beams is 2–3 orders of magnitude lower than that for common polymeric materials. The fact that it was possible to sputter quickly through the silicate layer suggests that the layer was very thin and/or only lightly oxidized, which is consistent with the low degree of cracking seen in the optical micrographs. The increase in the amount of PDMS at the interface relative to the bulk catheter indicates that this area is dominated by highly mobile low molecular weight PDMS oligomers that give a more intense SIMS signal than the crosslinked polymer. The presence of the low molecular weight PDMS at the interface is consistent with the relatively low dry measured mechanical strength of this sample.
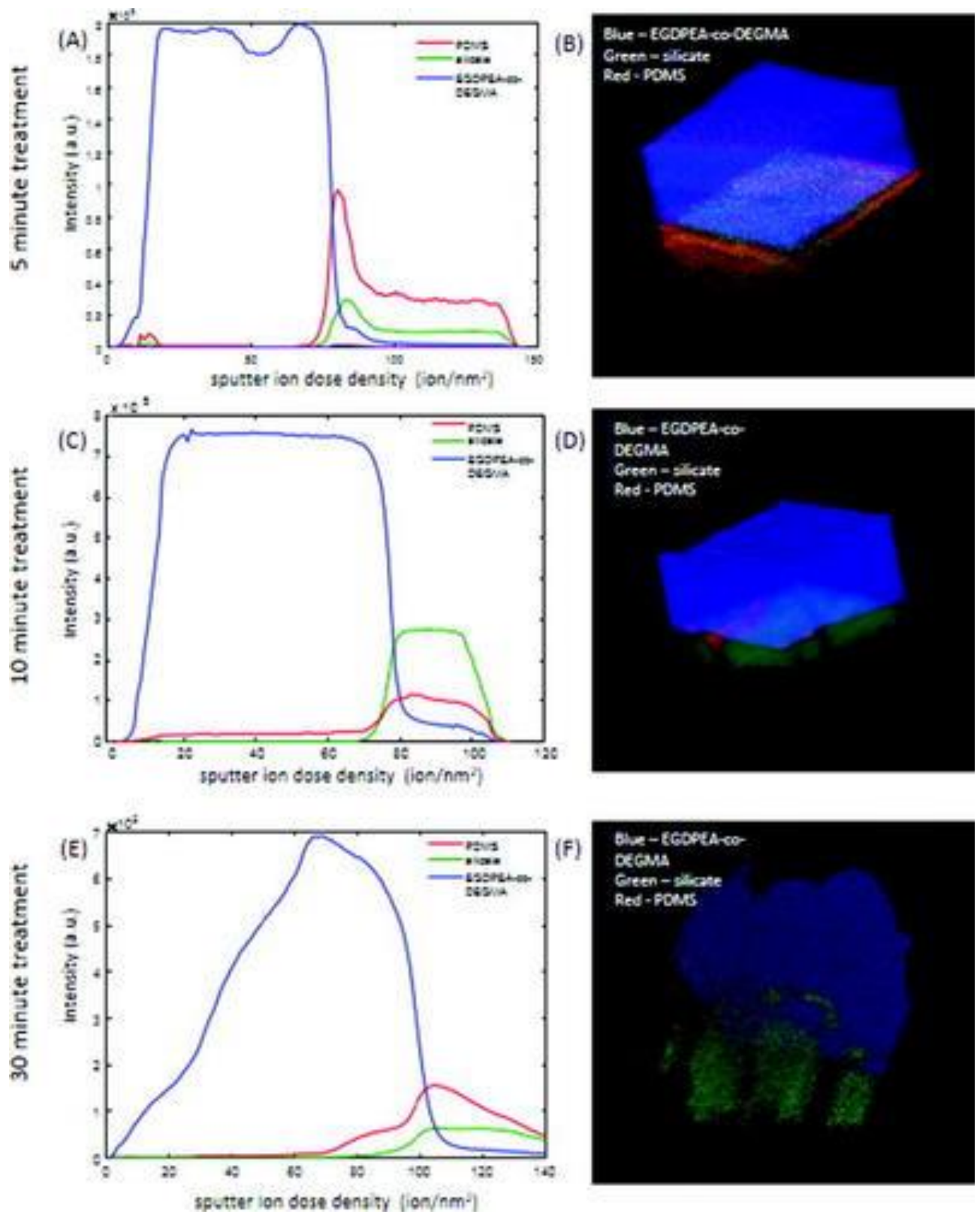
Figure 7. ToF-SIMS depth profiles and 3D images of 100×100 μm regions on EGDPEA-co-DEGMA coated PDMS catheters that were treated for 5 min. [(a) and (b)], 10 min [(c) and (d)], and 30 min [(e) and (f)] with the O2 plasma. EGDPEA-co-DEGMA is shown in blue, silicate in green, and PDMS in red. The depth scale is uncalibrated. The intensity is in arbitrary units.

In the samples treated for 10 and 30 minutes [figs. 7(c)-7(f)], the bulk PDMS catheter is never reached during the depth profiling, indicative of a thicker and/or harder silicate layer that is difficult to sputter. In the 10 min. samples, only two layers are observed, the EGDPEA–co-DEGMA film and a mixed silicate/PDMS layer. The PDMS signal rises only after the silicate signal appears (fig. 8A) and is observed along well defined cracks in the silicate layer (fig. 8B).

In contrast to the 10 min. sample, the PDMS signal in the 30 min. sample begins to increase well before the silicate signal appears [fig 7(e)], indicating the presence of an intermediate layer of mixed PDMS/EGDPEA–co-DEGMA. The 3D image [fig 7(f)] shows that this PDMS/EGDPEA–co-DEGMA layer is not uniform across the surface but is localized to particular areas. In the regions, where the PDMS extends up into the EGDPEA–co-DEGMA film, EGDPEA–co-DEGMA and PDMS are both present, indicating the two polymers are mixed at the resolution of the SIMS measurement (2-3 μm). Note that these mixed layers could be protruding down into cracks in the silicate layer rather than upward into the EGDPEA–co-DEGMA. It is impossible to distinguish these two possibilities from the SIMS measurement alone. The presence of PDMS between the polymer and the silicate layer is consistent with the higher water contact angle measured on this sample. For the 3D image [fig 7(f)], it is evident that the EGDPEA–co-DEGMA layer in this sample has more variation in thickness than for the previous samples. In general, the film is thinner in areas where there is more PDMS at the interface. This is consistent with the thinner average thickness determined by gravimetric analysis.

Figure 8 shows side-by-side comparison of the interface region (100 μm x 100 μm) for the same 5, 10 and 30 min. plasma treated samples shown in figure 7. In all three images, PDMS is shown in red, silicate is shown in green and salt-rich dust particles are shown in blue. The morphology of the interface in the 5 min. sample (fig. 8A) differs distinctly from the longer treatments. Not only is the silicate layer thinner and more easily sputtered, it is patchy and PDMS is visible across most of the interface. For the 10 min. treatment (fig. 8B), the PDMS appears only along distinct lines with nearly uniform width of ~10 μm. In the 30 min. treatment (fig. 8C), more of the interface is covered with PDMS and the features are much more irregular in size. Although this set of images shows an increasing number of particles at the interface with increasing plasma exposure time, replicate measurements showed significant region-to-region variability in the particle numbers.
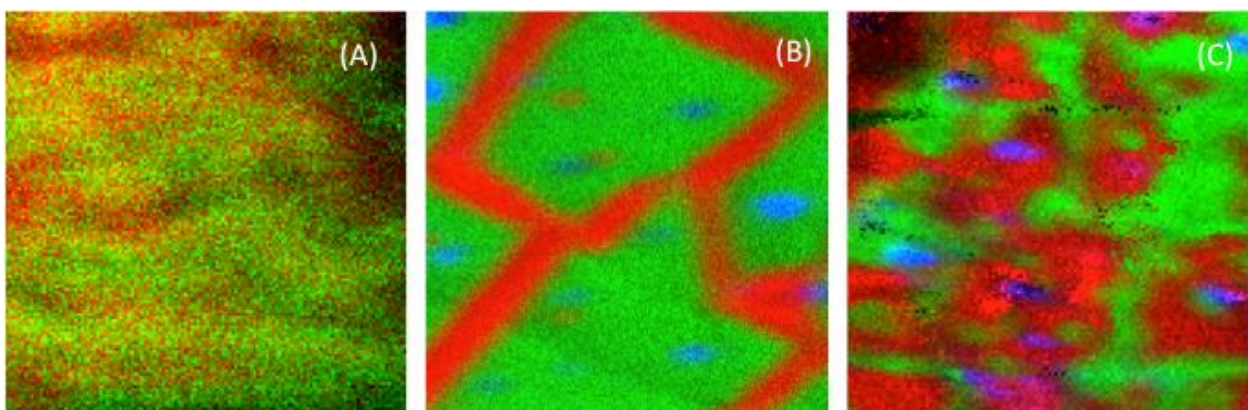

Figure 8. ToF-SIMS images of 100 ×100 μm of the interface between the EGDPEA-*co*-DEGMA coating and the plasma treated catheter surface. Samples plasma treated for 5 min (a), 10 min (b), and 30 min (c). Silicate is shown in green, PDMS is shown in red, and dust particles are shown in blue.

ToF-SIMS images collected following the depth profiles, after the argon cluster sputtering was stopped, showed rapid migration of the PDMS across the sputter cleaned surface. Figure 9 shows higher spatial resolution (~500 nm) ToF-SIMS images of the PDMS (m/z =73 + m/z = 147) signal of the interface of a second 10 min. treated area. The image on the left (fig. 9A) was completed within 1 minute of Ar cluster sputtering. The image on the right (fig. 9B) was taken 5 minutes later. As is evident from the images, PDMS migration across the sputter cleaned surface is very rapid with ~85% surface coverage occurring in 5 minutes. These results suggest that the uniform width of the PDMS lines in the 10 min. samples (fig. 8B) were the result of PDMS migration from cracks in the silicate during image acquisition between sputter cycles. To confirm this hypothesis, an additional ToF-SIMS depth profile was performed on the 10 min. catheter, while maintaining the sample at -130°C to prevent PDMS migration. In this depth-profile (data not shown) PDMS was still observed on the outermost surface but no PDMS was observed at the EGDPEA–co-DEGMA-silicate interface until the sample was allowed to warm up to ambient temperature and migration ensued.
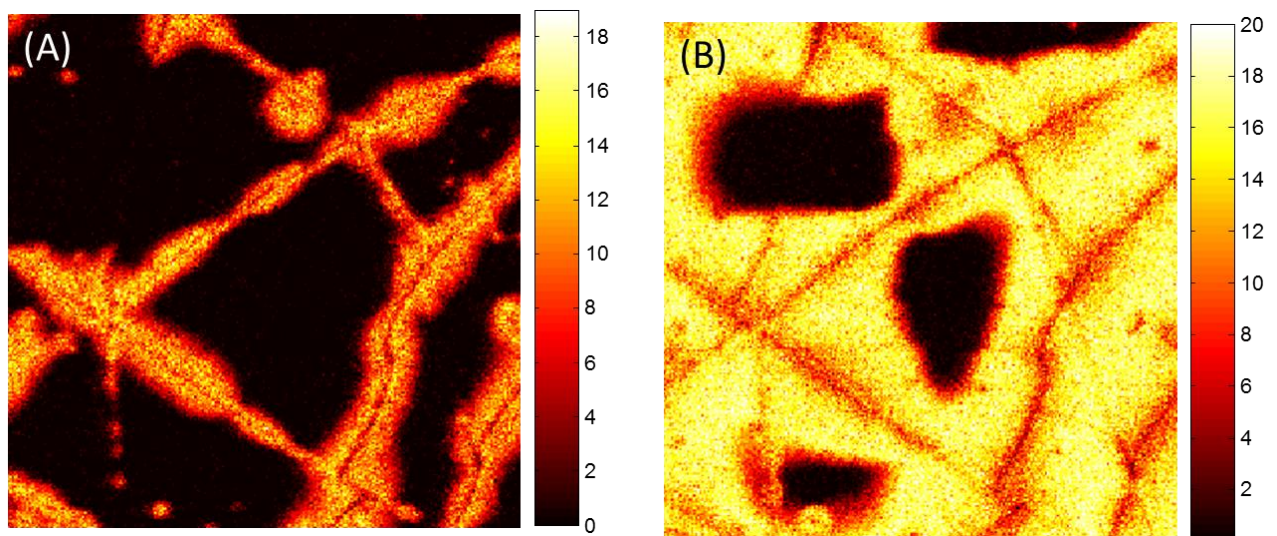

Figure 9. High spatial resolution 100 × 100 μm ToF-SIMS images of PDMS (m/z = 73) + (m/z = 147) at the coating/catheter interface taken immediately after 10 keV Ar sputtering (a) and 5 min after sputtering (b) for the sample that had been treated for 10 min with the O_2 plasma.

Figure 10 shows the results for ToF-SIMS analysis of the hydrated 10 min. treated catheter. This catheter was selected for the hydrated analysis because of the large (3 orders of magnitude) drop in RTD in the presence of water. In figure 10, EGDPEA–co-DEGMA is shown in red, silicate in green and water in blue. PDMS was not observed either at the surface or the interface of the hydrated sample. Once again, the 3D image has been corrected to align the base of the EGDPEA–co-DEGMA layer. As is evident in the depth profile (fig. 10A) and the 3D-image (fig. 10B), there is a large film of water between the EGDPEA–co-DEGMA layer and the silicate. The image of the interface (fig. 10C) shows beads of water (blue) separated by the cracks in the silicate. Although the EGDPEA–co-DEGMA layer itself does not pick up measurable water, water is able to permeate through the film to the hydrophilic interface. This likely disrupted the PDMS-coating interactions, which lead to the drop in RTD.
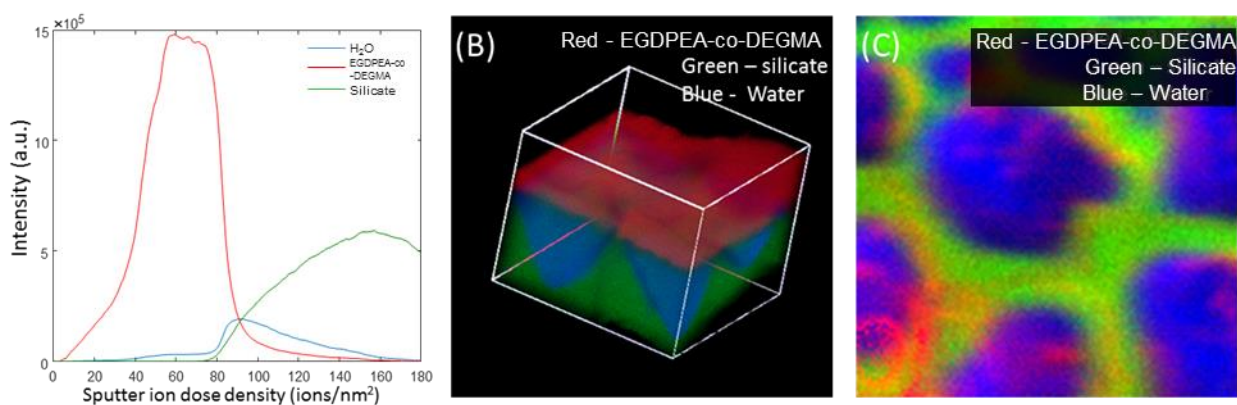
Figure 10: ToF-SIMS depth profile (A) and 3D image (B) and interface image (C) of 100 × 100 μm region of the hydrate 10 minute treatment EGDPEA-co-DEGMA coated PDMS catheter. EGDPEA-co-DEGMA is shown in red, silicate in green and water in blue.

Because the mechanical strength of the EGDPEA–CO-DEGMA/PDMS bond was found to be insufficient using only O_2 plasma treatment we utilised silanization as a methodology for improving interfacial interactions. An additional set of samples were prepared by priming with a mixture of tetrabutyl-titanate, tetrapropylsilicate and tetra (2-methoxyethoxy) silane in naphtha solvent. The primed coating showed dramatically improved adhesion under hydrated conditions, resisting 1000 rotations before delamination. Figure 11 summarizes results of the ToF-SIMS measurements on the dry primed sample. EGDPEA–co-DEGMA is shown in blue, silicate in green, primer in red, and PDMS in cyan. For simplicity, only the EGDPEA–co-DEGMA, silicate and primer are shown in the 3D image. Although peaks from the organic components of the primer overlapped with peaks from the polymer and the PDMS, the primer could be clearly identified by its unique titanium signal (see Table S1, supplemental information). The outermost surface of the primed catheter was contaminated with salt particles in all the regions imaged. These particles resulted in artefacts in the profile through the EGDPEA–co-DEGMA layer due to differential sputtering. These artefacts are evident in the dark regions in the 3D image and the remnants of EGDPEA–co-DEGMA that persist beyond the interface. Despite these artefacts, the primer, silicate and PDMS could all be identified in particle free regions of the sample.
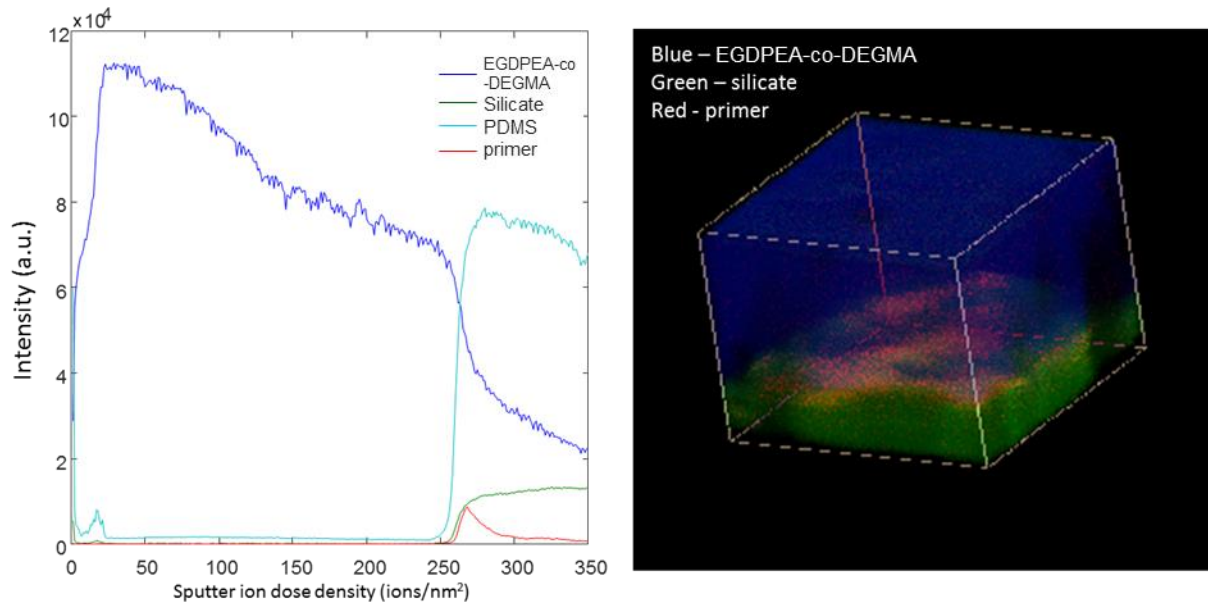
Figure 11: ToF-SIMS depth profile (A) and 3D image (B) of 100 × 100 μm region of EGDPEA-co-DEGMA coated PDMS catheter with Nusil primer. EGDPEA-co-DEGMA is shown in blue, silicate in green and primer in red. The depth scale is uncalibrated.

Figure 12 summarizes the cryo-ToF-SIMS results for the hydrated primed sample. Note that EGDPEA–co-DEGMA is shown in red in the 3D image (fig. 12 B) while primer is shown in red in the interface image (fig. 12 C). Although the primed sample showed significantly improved adhesion hydrated, trace amounts of water were observed at the interface between the EGDPEA–co-DEGMA and silicate. This trace amount of water was localized in a few discrete spots. Detailed analysis of spectra from these water containing regions showed salt and organic impurities that were not observed in the hydrated material without primer. This suggests that the traces of water were associated with hydrophilic salt particles that were seen at most of the interfaces.
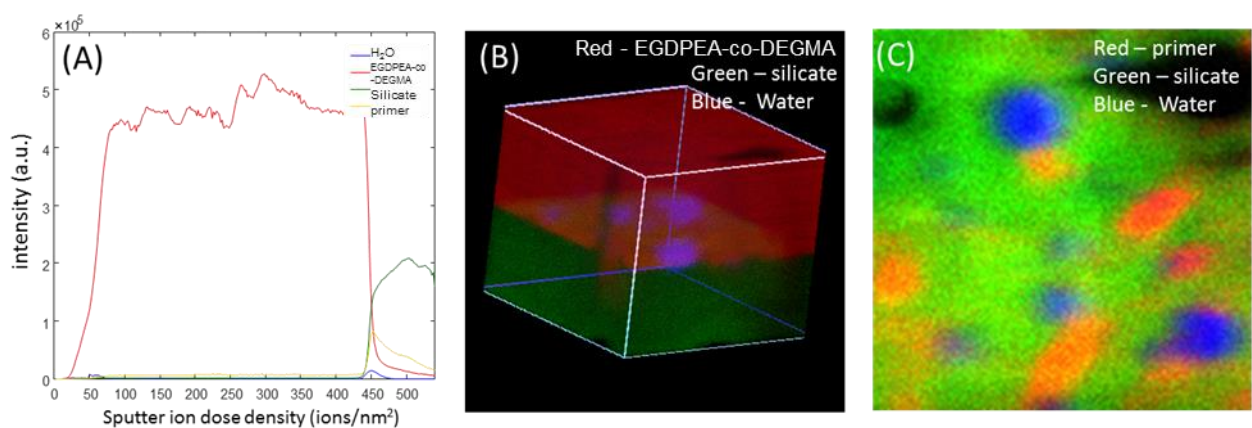

Figure 12: ToF-SIMS depth profile (A) and 3D image (B) and interface image (C) of 100 × 100 μm region of EGDPEA-co-DEGMA coated PDMS catheter that was treated for 5 min. with O2 plasma and then coated with primer. Note that in the 3D image (B), the EGDPEA-co-DEGMA coated is shown in red while in the interface image (C), red is used for the primer.

Clear differences in the levels of PDMS at the interface as well as the thickness and morphology of the silicate layer were detected for samples treated with the O2 plasma for 5, 10, and 30 min. The sample treated for 5min showed higher levels of hydrophobic PDMS at the interface, which could explain both the lower dry RTD values and the lower susceptibility of the adhesive bond to hydration.

The 10 min treated sample showed no PDMS at the interface although PDMS was able to migrate from the bulk to cover the bare silicate surface within a few min, once the EGDPEA-co-DEGMA film was removed. Although hydrophobic recovery of plasma-treated PDMS has been widely reported in the literature, it has generally been reported over periods of days not minutes.[27-28, 35-36] In this study, hydrophobic recovery on the uncoated plasma treated samples was observed after 1 week, but not in the measurements taken within 5 min of the treatment, in contrast to the SIMS results on sputter cleaned surfaces. This suggests that the rate of hydrophobic recovery is initially determined by the rate of crack propagation through the silicate layer. However, once cracks are formed, low molecular weight PDMS is able to rapidly migrate across the bare silicate surface in only a few min. The application of the EGDPEA-co-DEGMA coating immediately after plasma treatment, before the cracks are fully formed, can preserve the hydrophilic surface, but removing the EGDPEA-co-DEGMA coating after the cracks are formed leads rapidly to the PDMS coverage of the surface. This has important implications for the process development as well as forensic investigation of delaminated coatings.

The ToF-SIMS measurement of the 30 min treated sample showed increased PDMS, which is consistent with the high WCA measured on these samples. This film also showed a greater variation in the thickness of the polymer coating, associated with the surface cracks and holes. This suggests that the thinner coating, observed using gravimetric analysis, was the result of incomplete wetting of the surface at a microscale.

Cryo-ToF-SIMS analysis of the hydrated 10 min treated catheter revealed water disrupting contacts between the silicate and the EGDPEA-co-DEGMA layer over large portions of the surface. This suggests that the strong adhesion when dry was due primarily to easily hydrolyzed polar and hydrogen bonding interactions rather than covalent bonds.

In contrast, the sample treated with the primer showed only traces of water at the interface, which were likely associated with hydrophilic particulate contaminants, such as salt. Detection of water at the interface using cryo-ToF-SIMS proves that water is able to permeate the EGDPEA-co-DEGMA layer and access the interface but does not disrupt the adhesive bonds. This suggests that covalent bonding may be involved although no direct evidence for covalent bonding was found in the ToF-SIMS data. Evidence that hydrophilic dust particles may attract water to the interface suggests that future improvements in adhesion may be possible by reducing particulate contamination.

4. Conclusions

Dual-beam 3D imaging ToF-SIMS, using a 10 keV Ar_{2000}^+ cluster sputter source and a 30 keV Bi_3^+ analysis beam, was able to provide detailed information on the adhesive interface between the EGDPEA-co-DEGMA coating and the PDMS catheter. The polymer coating, PDMS, silicate, primer, and particulate contamination were identifiable in the interfacial region after sputtering through multiple micrometers of the polymer overlayer. Key components of the interface could be identified even in the presence of differential sputtering artefacts associated with surface particle contamination.

Oxygen plasma treatment of the PDMS catheter for 5–10 min resulted in efficient wetting of the catheter by the EGDPEA-co-DEGMA coating and good adhesion between the layers under dry conditions. Unfortunately, hydration, which is unavoidable in a urinary catheter, dramatically reduced the strength of the adhesive bond between the layers. Inclusion of a primer layer resulted in a more resilient adhesive bond between the EGDPEA-co-DEGMA and the PDMS catheter that was resistant to hydration. Although cryo-ToF-SIMS measurements could not directly confirm covalent bonding between the primed catheter and the coating, the ToF-SIMS measurements verified that adhesion persisted despite the presence of water at the interface. The resulting catheter material is resistant to bacterial biofilm colonization and has the mechanical properties necessary for use as a urinary catheter. Biofilm formation was reduced by between 86% and 95% in bacterial coverage for both *P. mirabilis* and UPEC compared to untreated PDMS and between 66% and 93% compared to the silver hydrogel after 10 days of continuous bacterial exposure. This study demonstrates the importance of Ar cluster depth profiling for the better understanding of adhesion between the polymeric layers and the development of improved biomaterials.

5.   Acknowledgements

6.   References

1.   Hooton, T. M.; Bradley, S. F.; Cardenas, D. D.; Colgan, R.; Geerlings, S. E.; Rice, J. C.; Saint, S.; Schaeffer, A. J.; Tambayh, P. A.; Tenke, P.; Nicolle, L. E., Diagnosis, Prevention, and Treatment of Catheter-Associated Urinary Tract Infection in Adults: 2009 International Clinical Practice Guidelines from the Infectious Diseases Society of America. *Clinical Infectious Diseases* **2010,** *50* (5), 625-663.
2.   Nicolle, L. E., Urinary catheter associated infections. *Infect Dis Clin North Am* **2012,** *26*.
3.   Zarb, P.; Coignard, B.; Griskevicienne, J.; Muller, A.; Vankerckho ven Weist, K.; Goossens, M. M.; Vaerenberg, S.; Hopkins, S.; Catry, B.; Monnet, D. L.; Goosens, H.; Suetens, C., The European Centre for Disease Prevention and Control (ECDC) pilot point prevalence survey of healthcare-associated infections and antimicrobial use. *Euro Surveill* **2012,** *17*.
4.   Chant, C.; Smith, D. M.; Marshall, J. C.; Friedrich, J. O., Relationship of catheter associated urinary tract infection to mortality and length of stay in critically ill patients: a systematic review and meta-analysis of observational studies. *Crit Care Med* **2011,** *39*.
5.   Kunin, C. M.; Chin, Q. F.; Chambers, S., Morbidity and mortality associated with indwelling urinary catheters in elderly patients in a nursing home – confounding due to the presence of associated diseases. *J Am Geriatr Soc* **1987,** *35*.
6.   Clec'h, C.; Schwebel, C.; Français, A.; Toledano, D.; Fosse, J.-P.; Garrouste-Orgeas, M.; Azoulay, E.; Adrie, C.; Jamali, S.; Descorps-Declere, A.; Nakache, D.; Timsit, J.-F.; Cohen, Y., Does Catheter-Associated Urinary Tract Infection Increase Mortality in Critically Ill Patients? *Infection Control & Hospital Epidemiology* **2007,** *28* (12), 1367-1373.
7.   Stickler, D. J.; Zimakoff, J., Complications of urinary tract infections associated with devices used for long-term bladder management. *J Hosp Infect* **1994,** *28*.
8.   Tenke, P.; Kovacs, B.; Bjerklund Johansen, T. E.; Matsumoto, T.; Tambyah, P. A.; Naber, K. G., European and Asian guidelines on management and prevention of catheter-associated urinary tract infections. *International Journal of Antimicrobial Agents* **2008,** *31, Supplement 1*, 68-78.
9.   Hook, A. L.; Chang, C. Y.; Yang, J.; Atkinson, S.; Langer, R.; Anderson, D. G.; Davies, M. C.; Williams, P.; Alexander, M. R., Discovery of novel materials with broad resistance to bacterial attachment using combinatorial polymer microarrays. *Adv Mater* **2013,** *25* (18), 2542-2547.
10.   Hook, A. L.; Chang, C.-Y.; Yang, J.; Luckett, J.; Cockayne, A.; Atkinson, S.; Mei, Y.; Bayston, R.; Irvine, D. J.; Langer, R.; Anderson, D. G.; Williams, P.; Davies, M. C.; Alexander, M. R., Combinatorial discovery of polymers resistant to bacterial attachment. *Nat Biotech* **2012,** *30* (9), 868-875.
11.   Adlington, K.; Nguyen, N. T.; Eaves, E.; Yang, J.; Chang, C.-Y.; Li, J.; Gower, A. L.; Stimpson, A.; Anderson, D. G.; Langer, R.; Davies, M. C.; Hook, A. L.; Williams, P.; Alexander, M. R.; Irvine, D. J., Application of

Targeted Molecular and Material Property Optimization to Bacterial Attachment-Resistant (Meth)acrylate Polymers. *Biomacromolecules* **2016,** *17* (9), 2830-2838.

12. Hook, A. L.; Chang, C.; Yang, J.; Luckett, J.; Cockrayne, A.; Atkinson, S.; Mei, Y.; Bayston, R.; Irvine, D. J.; Langer, R.; Anderson, D. G.; Williams, P.; Davies, M. C.; Alexander, M. R., Combinatorial discovery of polymers resistant to bacterial attachment. *Nature Biotechnology* **2012,** *30* (9), 868-875.

13. Leung, J. M.; Berry, L. R.; Chan, A. K. C.; Brash, J. L., Surface modification of polydimethylsiloxane with a covalent antithrombin-heparin complex to prevent thrombosis. *Journal of Biomaterials Science-Polymer Edition* **2014,** *25* (8), 786-801.

14. Williams, R. L.; Wilson, D. J.; Rhodes, N. P., Stability of plasma-treated silicone rubber and its influence on the interfacial aspects of blood compatibility. *Biomaterials* **2004,** *25* (19), 4659-4673.

15. Abbasi, F.; Mirzadeh, H.; Katbab, A.-A., Modification of polysiloxane polymers for biomedical applications: a review. *Polymer International* **2001,** *50* (12), 1279-1287.

16. Ratner, B. D.; Hoffman, A.; Whiffen, J., The thrombogenicity of radiation grafted polymers as measured by the vena cava ring test. *Journal of bioengineering* **1978,** *2* (3-4), 313-323.

17. Gengenbach, T. R.; Chatelier, R. C.; Griesser, H. J., Characterization of the ageing of plasma-deposited polymer films: Global analysis of X-ray photoelectron spectroscopy data. *Surface and Interface Analysis* **1996,** *24* (4), 271-281.

18. Parvin, A.; Mirzadeh, H.; Khorasani, M. T., Physicochemical and biological evaluation of plasma-induced graft polymerization of acrylamide onto polydimethylsiloxane. *Journal of Applied Polymer Science* **2008,** *107* (4), 2343-2349.

19. Seah, M.; Spencer, S.; Havelund, R.; Gilmore, I.; Shard, A., Depth resolution at organic interfaces sputtered by argon gas cluster ions: the effect of energy, angle and cluster size. *Analyst* **2015,** *140* (19), 6508-6516.

20. Angerer, T. B.; Blenkinsopp, P.; Fletcher, J. S., High energy gas cluster ions for organic and biological analysis by time-of-flight secondary ion mass spectrometry. *Int J Mass Spectrom* **2015,** *377*, 591-598.

21. Mahoney, C. M.; Wucher, A., Molecular Depth Profiling with Cluster Ion Beams. *Cluster Secondary Ion Mass Spectrometry: Principles and Applications* **2013**, 117-205.

22. Körsgen, M.; Pelster, A.; Dreisewerd, K.; Arlinghaus, H. F., 3D ToF-SIMS Analysis of Peptide Incorporation into MALDI Matrix Crystals with Sub-micrometer Resolution. *Journal of The American Society for Mass Spectrometry* **2016,** *27* (2), 277-284.

23. Pelster, A.; Tyler, B. J.; Stover, M.; Unger, W. E. S.; Arlinghaus, H. F., Improved 3D-imaging of a sirolimus/probucol eluting stent coating using laser postionization secondary neutral mass spectrometry and time-of-flight secondary ion mass spectrometry. *Biointerphases* **2016,** *11* (4), 041001.

24. Rading, D.; Moellers, R.; Cramer, H. G.; Niehuis, E., Dual beam depth profiling of polymer materials: Comparison of C60 and Ar cluster ion beams for sputtering. *Surface and Interface Analysis* **2013,** *45* (1), 171-174.

25. Berger, H.; Hacker, J.; Juarez, A.; Hughes, C.; Goebel, W., Cloning of the chromosomal determinants encoding hemolysin production and mannose-resistant hemagglutination in Escherichia-coli. *J Bacteriol.* **1982,** *152* (3), 1241-1247.

26. Fritz, J. L.; Owen, M. J., Hydrophobic recovery of plasma-treated polydimethylsiloxane. *Journal of Adhesion* **1995,** *54* (1-2), 33-45.

27. Hillborg, H.; Ankner, J. F.; Gedde, U. W.; Smith, G. D.; Yasuda, H. K.; Wikstrom, K., Crosslinked polydimethylsiloxane exposed to oxygen plasma studied by neutron reflectometry and other surface specific techniques. *Polymer* **2000,** *41* (18), 6851-6863.

28. Karkhaneh, A.; Mirzadeh, H.; Ghaffariyeh, A. R., Simultaneous graft copolymerization of 2-hydroxyethyl methacrylate and acrylic acid onto polydimethylsiloxane surfaces using a two-step plasma treatment. *Journal of Applied Polymer Science* **2007,** *105* (4), 2208-2217.

29. Hidron, A. I.; Edwards, J. R.; Patel, J.; Horan, T. C.; Sievert, D. M.; Pollock, D. A.; Fridkin, S. K.; Natl Healthcare Safety Network, T.; Participating Natl Healthcare, S., Antimicrobial-Resistant Pathogens Associated With Healthcare-Associated Infections: Annual Summary of Data Reported to the National Healthcare Safety Network at the Centers for Disease Control and Prevention, 2006-2007. *Infection Control and Hospital Epidemiology* **2008,** *29* (11), 996-1011.

30. Schumm, K.; Lam, T. B., Types of urethral catheters for management of short-term voiding problems in hospitalised adults. *Cochrane Database Systematic Reviews* **2008,** *16* (2), CD004013.

31. Robinson, M. A.; Graham, D. J.; Castner, D. G., ToF-SIMS Depth Profiling of Cells: z-Correction, 3D Imaging, and Sputter Rate of Individual NIH/3T3 Fibroblasts. *Analytical Chemistry* **2012,** *84* (11), 4880-4885.

32. Breitenstein, D.; Rommel, C. E.; Mollers, R.; Wegener, J.; Hagenhoff, B., The chemical composition of animal cells and their intracellular compartments reconstructed from 3D mass spectrometry. *Angew Chem Int Ed Engl* **2007,** *46* (28), 5332-5.

33. Peterson, R.; Tyler, B., Surface composition of atmospheric aerosol: individual particle characterization by TOF-SIMS. *Applied surface science* **2003,** *203*, 751-756.

34. Peterson, R. E.; Tyler, B. J., Analysis of organic and inorganic species on the surface of atmospheric aerosol using time-of-flight secondary ion mass spectrometry (TOF-SIMS). *Atmospheric Environment* **2002,** *36* (39-40), 6041-6049.

35. Roth, J.; Albrecht, V.; Nitschke, M.; Bellmann, C.; Simon, F.; Zschoche, S.; Michel, S.; Luhmann, C.; Grundke, K.; Voit, B., Surface Functionalization of Silicone Rubber for Permanent Adhesion Improvement. *Langmuir* **2008,** *24* (21), 12603-12611.

36. Rangel, E. C.; Gadioli, G. Z.; Cruz, N. C., Investigations on the stability of plasma modified silicone surfaces. *Plasmas and Polymers* **2004,** *9* (1), 35-48.

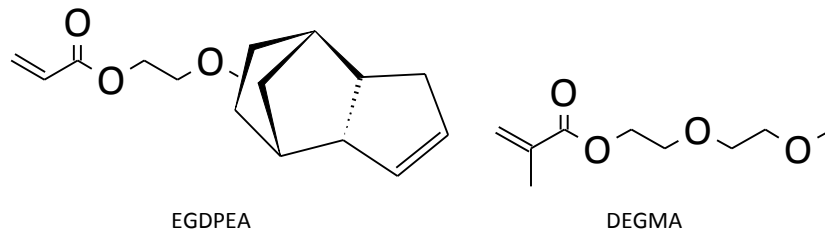EGDPEA   DEGMA

Figure S1: Chemical structures of the ethylene glycol dicyclopentenyl ether acrylate (EGDPEA) and di(ethyleneglycol) methyl ether methacrylate (DEGMA), which were copolymerized to make the bacterial resistant biofilm polymer.
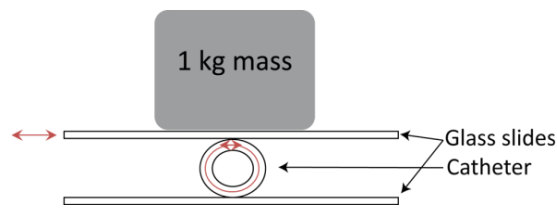

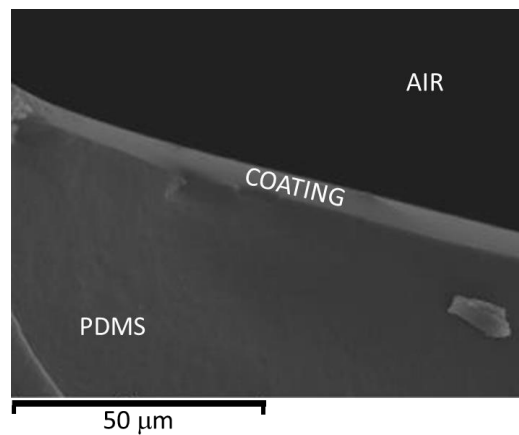Figure S2: Schematic depiction of the revolutions-to-delamination (RTD) assay.

Figure S3: Representative SEM image of the EGDPEA-co-DEGMA film on the treated PDMS catheter tubing. PDMS, coating and air regions are indicated on the image.
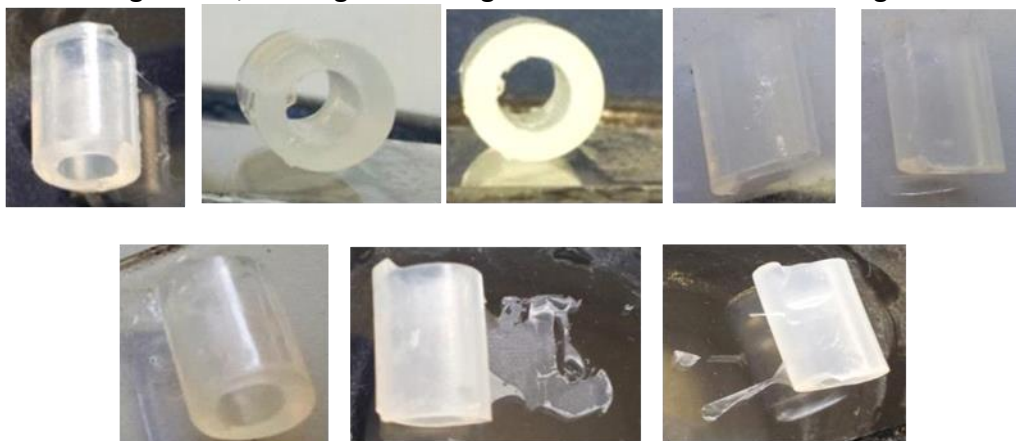
Figure S4: Examples of delamination of the EGDPEA-co-DEGMA film from the treated PDMS catheter tubing
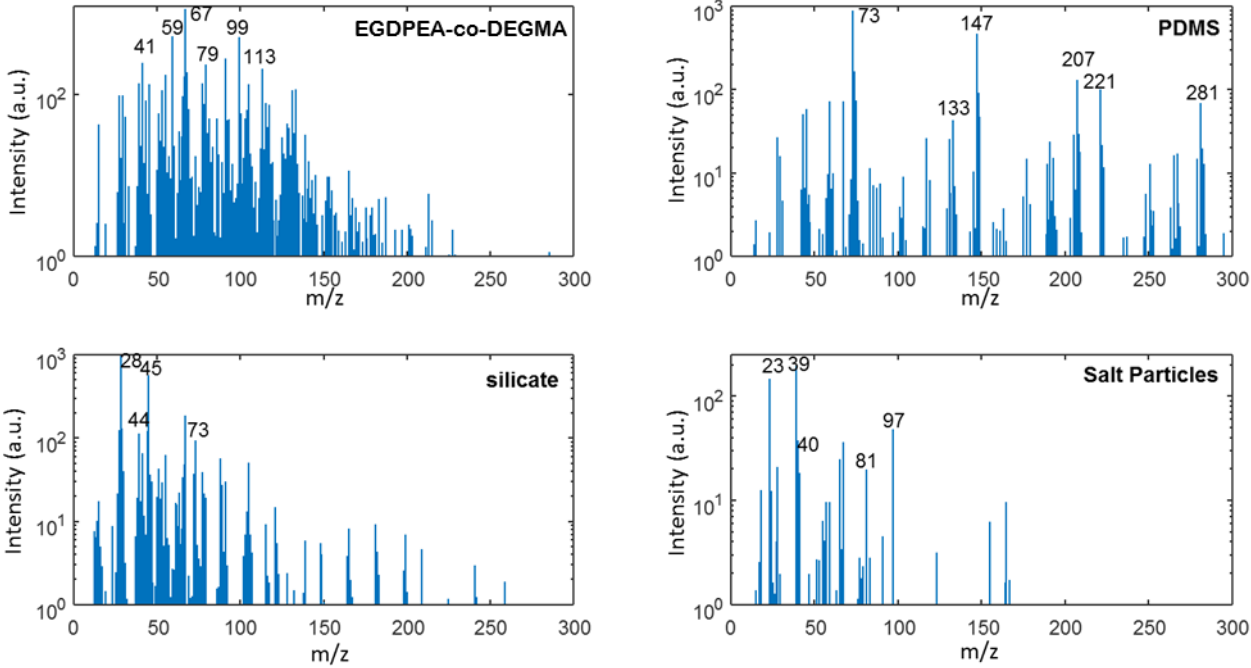

Figure S5: Spectra of the major components identified in the EGDPEA-co-DEGMA coated PDMS catheter samples

Table S1: Characteristic Ions

Component	m/z	Formula
EGDPEA–co-DEGMA	41.04	$C_3H_5^+$
	59.05	$C_3H_7O^+$
	67.05	$C_5H_7^+$
	79.05	$C_6H_7^+$
	99.04	$C_5H_7O_2^+$
	113.06	$C_6H_9O_2^+$
PDMS	73.05	$SiC_3H_9^+$
	147	$Si_2OC_5H_{15}^+$
	207.07	$Si_3O_2C_6H_{19}^+$
	221.08	$Si_3O_2C_7H_{21}^+$
silicate	27.98	Si^+
	44.98	$SiOH^+$
Salts	18.03	NH_4^+
	22.99	Na^+
	38.96	K^+
	39.96	Ca^+
	40.96	$^{41}K^+$
	80.95	Na_2Cl^+
	97.92	$KNaCl^+$
water		
	37.03	$H_5O_2^+$
Ti	47.95	Ti^+
	63.94	TiO^+